BMC Plant Biology

RESEARCH Open Access

Genome-wide identification of NDR1/HIN1-like genes in kiwifruit and function analysis of *AeNHL17* in response to disease resistance

Min Zhang[1,2], Rong Fu[1], Miao-Miao Lin[1,2], Jin-Bao Fang[1], Ran Wang[1], Yu-Kuo Li[1,2], Jin-Yong Chen[1], Lei-Ming Sun[1*] and Xiu-Juan Qi[1,2*]

Abstract

Background NDR1/HIN1-like (*NHL*) genes play crucial roles in Psa resistance. Kiwifruit canker, caused by *Pseudomonas syringae* pv. *Actinidiae* (Psa) infection is one of the most serious diseases affecting the kiwifruit industry. However, the key *NHL* has not yet been identified in kiwifruit.

Results In this study, we conducted a genome-wide identification of *NHL* family in kiwifruit (*Actinidia eriantha*). A total of 33 *AeNHLs* were divided into five domain-conserved subfamilies, which were mainly assigned into phytohormones and defense responses. The expression of *AeNHL* genes was analyzed to identify key genes in response to Psa, and we found *AeNHL17* was highly expressed upon Psa inoculation. Transgenic tobacco overexpressing *AeNHL17* presented higher resistance to Psa than wild-type (WT) tobacco, implying a key role for *AeNHL17* in Psa resistance. Finally, we carried out a stable genetic transformation of kiwifruit (*A. chinensis*), which is sensitive to Psa, and found that the overexpression of *AeNHL17* increased resistance to infection. *AeNHL17*-silenced plants exhibited larger disease lesions than control plants.

Conclusions Our findings revealed the function of *AaNHL17* in Psa resistance, providing new data regarding the functional analysis of the *NHL* gene family in kiwifruit.

Keywords NDR1/HIN1-like gene family, Kiwifruit, Psa, AeNHL17, Disease resistance

Introduction

Kiwifruit (*Actinidia* spp.) is native to China and is a rich germplasm resource with a wide geographical distribution. It is a domesticated fruit plant and has become an important horticultural crop [1, 2]. However, kiwifruit bacterial canker (KBC) caused by *Pseudomonas syringae* pv. *Actinidae* (Psa) have led to devastation of the kiwifruit industry worldwide [3–5]. This disease was first reported in Japan and was later discovered in China and other kiwifruit-producing areas such as Italy, Korea, and New Zealand [6–9]. KBC is gradually becoming the primary factor limiting the kiwifruit industry development globally [10]. The currently discovered Psa lines can be

*Correspondence:
Lei-Ming Sun
sunleiming@caas.cn
Xiu-Juan Qi
qixiujuan@caas.cn
[1]National Key Laboratory for Germplasm Innovation & Utilization of Horticultural Crop/ Zhengzhou Fruit Research Institute, Chinese Academy of Agricultural Sciences, Zhengzhou 450009, China
[2]Zhongyuan Research Center, Chinese Academy of Agricultural Sciences, Xinxiang 453514, China

divided into four types based on genomic comparison, phylogeny, and origin [11]. The Psa biovar is highly virulent, and once it systemically invades a plant, it may quickly lead to plant death [12]. Therefore, exploring the disease defense mechanisms of kiwifruit is crucial for preventing Psa infections.

Plants have evolved sophisticated regulatory networks to resist infection, such as PAMP-triggered immunity (PTI), effector-triggered immunity (ETI), hypersensitive response (HR), and systemic acquired resistance (SAR) [13, 14]. PTI and ETI are basic defense responses when plants face environmental attacks. Further pathogen resistance mediated by resistance genes, is usually associated with HR and SAR [15]. These processes require the tight coordination of multiple phytohormones, including jasmonic acid (JA), ethylene (ET) and salicylic acid (SA) [16]. Previous studies have shown that the pathogen infection response can increase the expression of the immune signal SA, which is usually consistent with the increased transcription level of pathogenesis-related (*PR*) genes and strengthens disease resistance [17, 18].

NDR1/HIN-like (*NHL*) genes are characterized by sequence and structural similarity to Non-race-specific disease resistance 1 (*NDR1*) of *Arabidopsis thaliana* and Harpin-induced 1 (*HIN1*) of *Nicotiana tabacum* [19, 20]. *NDR1* is necessary for resistance genes to recognize pathogens and plays a role in plant disease resistance responses by encoding plasma membrane-localized proteins [20]. *HIN1* is triggered by pathogens and plays critical roles in the plant defense pathway [21]. Most NHL proteins have two highly conserved motifs, including a conserved late embryogenesis abundant (LEA) domain [22]. The LEA domain belongs to a protein family involved in osmotic regulation, and these proteins typically participate in protecting plants from biotic and abiotic damage [23].

Previous studies have shown that *NHL* genes play an important role in plant-pathogen interactions and resistance to abiotic stress [22, 24]. For example, the expression of *NHL3* is significantly induced by a variety *Pseudomonas* strains in *Arabidopsis*, and the overexpression of *NHL3* strengthens plant resistance to *Pseudomonas syringae* pv. *tomato* DC3000 [22, 25]. The hypersensitive response of *NHL10* cells to *Cucumber mosaic virus* (CMV) infection is controlled by the SA signaling pathway [26]. Similarly, the overexpression of *StPOTHR1* can strengthen resistance against *P. infestans* in potatoes [27]. In pepper, transient overexpression of *CaNHL4* increases plant resistance, and *CaNHL4*-silenced plants show significantly increased susceptibility to different pathogens [28]. Overall, these studies demonstrate that *NHL* family members identified from different plants play essential roles in resistance and stress responses to pathogen infection. However, the *NHL* gene family in kiwifruit and its function in response to biotic and abiotic stress remain largely unknown.

In the present study, we identified the *NHL* gene family based on whole-genome sequences of *A. eriantha*. The phylogenetic relationships, chromosomal localization, and other structural features of AeNHLs were analyzed systematically. Subsequently, we isolated an *NHL* gene *AeNHL17* which is highly similar to pathogen resistance-related *NHLs* from other species. The function of *AeNHL17* has been characterized in transgenic tobacco and kiwifruit plants. These findings provide evidence for further studies on the function of *NHL* in kiwifruit disease resistance and provide new genes for resistance breeding.

Results

Identification of AeNHLs in *A. eriantha*

To determine the *NHL* gene family in *A. eriantha*, 45 NDR1/HIN1-like sequences from *A. thaliana* were used as queries for BLAST search in Kiwifruit Genome Database. The BLAST search results were refined by manual selection to remove redundant sequences, and SMART was used to confirm the presence of the LEA-2 domain (PF03168). Table 1 shows that a total of 33 *AeNHL* genes were acquired, which were named *AeNHL1* to *AeNHL33* based on the reference genome localization. The CDS lengths of *AeNHLs* was 573 bp (*AeNHL7*) to 1614 bp (*AeNHL13*) (Table 1). The molecular weights (MW) were in the range of 20.55 to 60.23 kDa, and the isoelectric point (pI) was in the range of 7.09 (*AeNHL30*) to 10.43 (*AeNHL21*) (Table 1).

Phylogenetic analysis and chromosome location of the AeNHLs

To understand the evolutionary relationship between NHL proteins, 27 AtNHL and 33 AeNHL proteins were used to perform sequence alignment and to construct an unrooted NJ tree. The total 60 NHL proteins were divided into five well-conserved subgroups (Fig. 1). Group I had the largest number and included nine AeNHL proteins, while Group V had the smallest number and contained three AeNHL proteins (Fig. 1). AeNHL17 and AeNHL10 were closer to AtNHL3. The login numbers of the NHL protein homolog sequences used in the unrooted NJ tree are listed in Supplementary Table S2.

The chromosomal localization of *AeNHLs* was further determined using a simplified physical map, which revealed that 33 *AeNHL* genes were unevenly distributed across 20 chromosomes in *A. eriantha* genome (Fig. 2). Chromosomes (Chr) 5, 6, 7, 18, 20, 21, 23, 25, 26, 27, and 0 contained one copy each; Chr3, 11, 14, 16, 19, and 28 contained two copies each; Chr 2 and 8 contained three copies each; and Chr 15 contained four copies.

Table 1 Characterization of identified *AeNHL* genes in *A. eriantha*

Name	Gene ID	Chromosome location	CDS (bp)	MW (kDa)	pI
AeNHL1	DTZ79_02g00550	LG2:472472–473,110	639	23.79	9.65
AeNHL2	DTZ79_02g01580	LG2:1280992–1,281,645	654	24.72	10.04
AeNHL3	DTZ79_02g07380	LG2:7318550–7,319,164	615	22.32	10.23
AeNHL4	DTZ79_03g00560	LG3:726701–727,339	639	23.66	9.43
AeNHL5	DTZ79_03g08330	LG3:8554895–8,555,527	633	23.76	9.73
AeNHL6	DTZ79_05g01590	LG5:2153616–2,154,368	753	28.43	9.86
AeNHL7	DTZ79_06g09910	LG6:16778957–16,779,943	573	20.55	9.21
AeNHL8	DTZ79_07g03930	LG7:4045388–4,047,763	594	21.32	8.96
AeNHL9	DTZ79_08g00870	LG8:1128557–1,133,851	624	23.31	10.09
AeNHL10	DTZ79_08g00880	LG8:1142089–1,142,784	696	26.43	9.51
AeNHL11	DTZ79_08g16200	LG8:27133049–27,134,597	819	30.79	9.27
AeNHL12	DTZ79_11g02010	LG11:2056415–2,059,016	969	35.30	9.86
AeNHL13	DTZ79_11g08930	LG11:14856415–14,864,364	1614	59.00	9.16
AeNHL14	DTZ79_14g04210	LG14:4840482–4,849,361	1602	59.10	10.12
AeNHL15	DTZ79_14g08860	LG14:13459555–13,460,278	651	24.12	10.17
AeNHL16	DTZ79_15g07790	LG15:10126568–10,129,976	867	32.63	9.87
AeNHL17	DTZ79_15g07880	LG15:10343397–10,352,083	696	26.54	9.45
AeNHL18	DTZ79_15g13030	LG15:17940403–17,945,263	1257	48.34	9.81
AeNHL19	DTZ79_15g13230	LG15:18066546–18,074,706	1587	60.24	10.01
AeNHL20	DTZ79_16g00990	LG16:1085317–1,086,881	882	33.20	8.90
AeNHL21	DTZ79_16g01530	LG16:1612922–1,613,673	726	26.23	10.43
AeNHL22	DTZ79_18g06590	LG18:14558202–14,562,670	861	32.38	9.84
AeNHL23	DTZ79_19g03750	LG19:11576715–11,580,733	615	21.85	8.95
AeNHL24	DTZ79_19g14810	LG19:24463556–24,465,866	885	32.74	9.05
AeNHL25	DTZ79_20g11920	LG20:18639964–18,642,612	900	33.27	8.84
AeNHL26	DTZ79_21g06400	LG21:7075917–7,076,969	957	34.88	8.81
AeNHL27	DTZ79_23g17320	LG23:21317601–21,321,313	924	33.96	9.80
AeNHL28	DTZ79_25g05970	LG25:15152300–15,155,603	801	29.17	9.71
AeNHL29	DTZ79_26g11040	LG26:18413635–18,416,550	774	28.40	9.56
AeNHL30	DTZ79_27g07370	LG27:8537730–8,538,593	864	31.30	7.09
AeNHL31	DTZ79_28g08090	LG28:12897954–12,900,898	1575	57.89	9.06
AeNHL32	DTZ79_28g08100	LG28:12904890–12,915,001	972	36.23	10.21
AeNHL33	DTZ79_00g01080	LG0:1911615–1,912,520	627	23.07	9.30

Analysis of cis-elements and conserved motifs in AeNHLs

To better understand the expression and regulation of *AeNHL* members, their promoter sequences were extracted and regulatory elements were explored. The results showed that more than 15 regulatory elements were abundant in the promoter regions of *AeNHLs*, including stress and defense response elements, light responsive elements, and hormone regulation elements, including auxin (IAA), methyl jasmonate (MeJA), abscisic acid (ABA), and gibberellin (GA) (Fig. 3a). Furthermore, we discovered that some AeNHL genes contained salicylic acid (SA)-responsive elements, indicating that these members may be involved in the SA-mediated responses. These results imply that the function of AeNHL proteins in kiwifruit may be related to disease resistance.

MEME motif analysis indicated that AeNHL proteins have two widely distributed motifs: motifs 1 and 3. Additionally, AeNHL members in the same phylogenetic subgroup had similar and specific motif sequences. For example, AeNHL1 and AeNHL4 were located in the same subgroup as motifs 1, 2, 3, 4, and 9 (Fig. 3b). The similarity in motifs between AeNHL proteins suggests that these protein structures are conserved in specific subgroups. Collectively, our results indicated that AeNHL proteins within the same subfamily have conserved motifs and domains, implying a similar potential role in kiwifruit disease defense.

Expression profiling of AeNHLs

Quantitative real-time RT-PCR was performed to explore the global expression profiles of *AeNHL* members during Psa infection. The expression of *AeNHL8*, *AeNHL9*, *AeNHL10*, *AeNHL*12, *AeNHL17* and *AeNHL*27 was significantly induced and rapidly increased, peaking at 12 h post-inoculation (Fig. 4). Conversely, the expression of some *AeNHL* genes decreased rapidly, whereas some members showed not expression (Supplementary Fig. S1). Expression levels of *AeNHL9*, *AeNHL10*, and

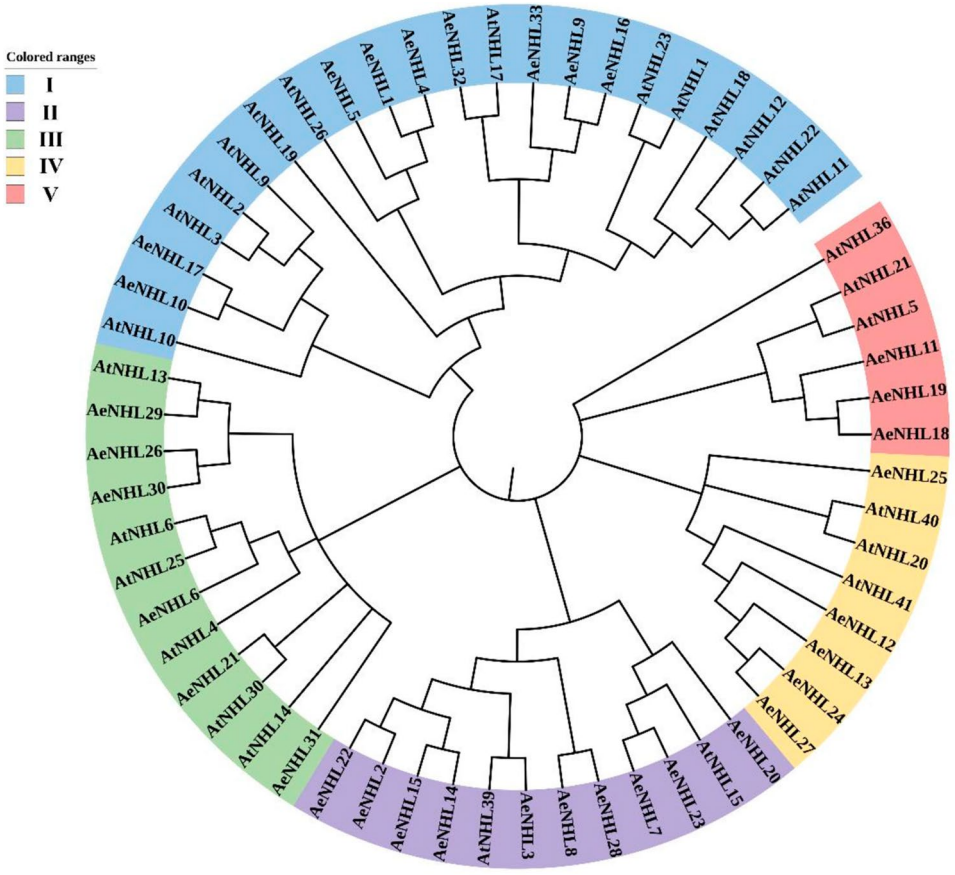

Fig. 1 Unrooted phylogenetic tree of NHL protein family from *A. eriantha* (Ae) and *A. thaliana* (At). MEGA 11.0.13 was used to construct the phylogenetic tree based on the NHL protein sequences, and the five distinct subgroups of NHL proteins were shown. iTOL [29] tool was used to annotate the phylogenetic tree

AeNHL17 in different tissues and floral organs were also investigated.

The results showed that these three genes were expressed in almost all the tissues and floral organs; however, their expression patterns differed. For instance, the expression of *AeNHL9* was the highest in flowers and the lowest in roots. *AeNHL17* showed the highest expression in mature stems and the lowest expression in buds (Fig. 5a-c). Among the floral organs, the highest levels of these three genes were observed in the sepals (Fig. 5d-f).

To further determine the temporal expression levels of *AeNHL17* in response to SA, MeJA, and ABA treatments, qRT-PCR was performed. As shown in Fig. 5g, *AeNHL17* expression gradually increased, with a single peak 12 h after the plants were treated with SA. Upon MeJA and ABA treatment, the transcription level of *AeNHL17* rapidly declined and minimum expression levels were observed at 12 h, after which it gradually increased and then peaked at 48 h (Fig. 5h-i).

Sequence analysis and subcellular localization of AeNHL17

To identify the potential functions of *AeNHL* gene family members, we selected *AeNHL17*, which is highly responsive to pathogens and SA stress for further study. The full length CDS of *AeNHL17* was 696 bp, encoding 231 amino acids with a pI of 9.45 and a MW of 26.5 kDa. Protein sequence and phylogenetic analysis showed that AeNHL17 had an LEA_2 domain and clustered with KAI7992218 from *Camellia lanceoleosa* (Fig. 6a-b).

To explore the subcellular localization of AeNHL17 protein, a pBWA(V)HS-AeNHL17-GFP fusion vector was constructed (Fig. 6c). The recombinant plasmid driven by CaMV 35 S promoter was transiently transformed into tobacco leaves. Two days after infiltration, confocal microscopy was used to visualize the green fluoresce signals of the cells. The AeNHL17 protein was located in the plasma membrane according to the green fluorescence signal (GFP). In contrast, the GFP signal from the control plasmid was distributed throughout the cells (Fig. 6d).

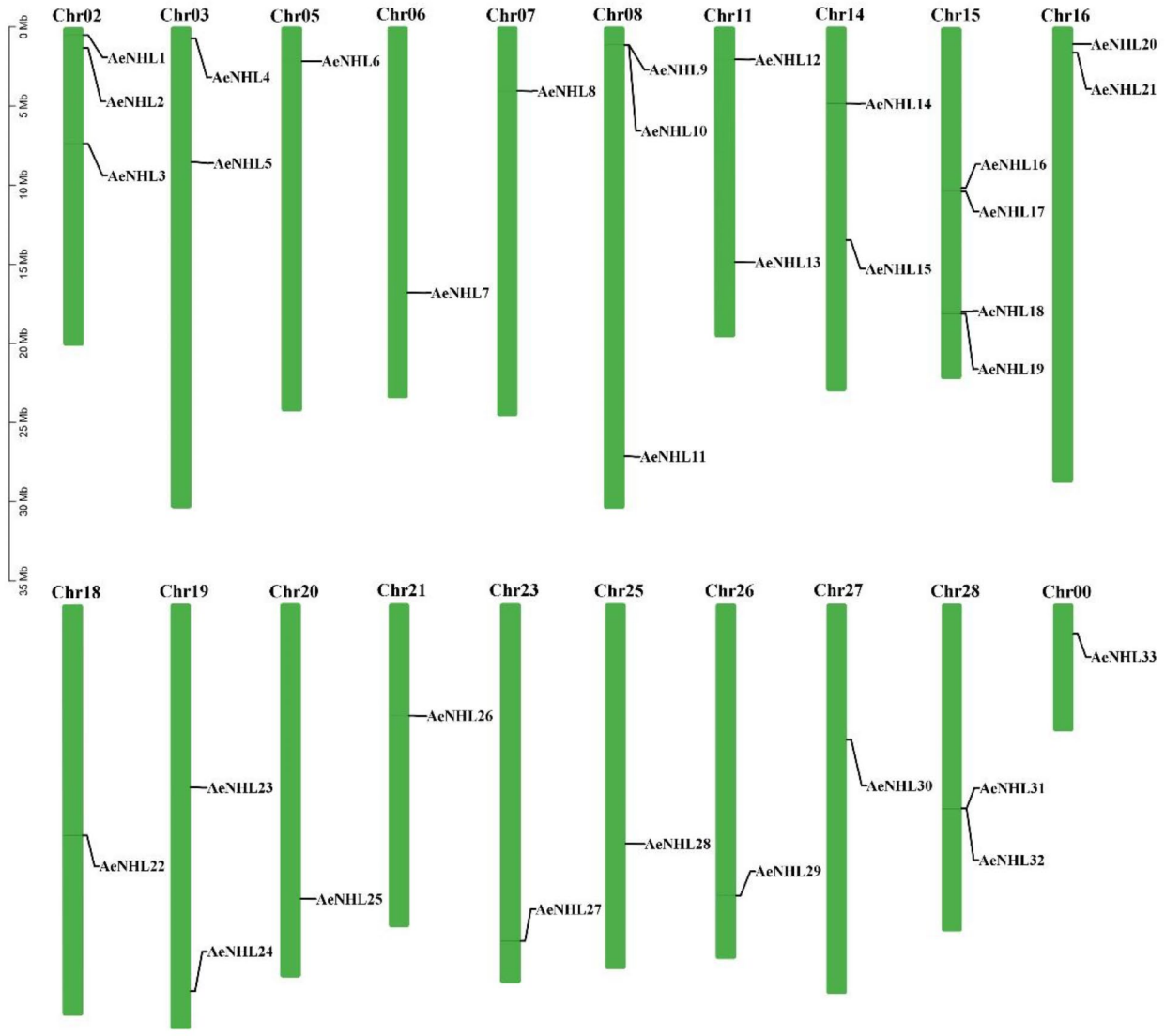

Fig. 2 Chromosomal positions of *AeNHL* genes. Chromosome numbers are indicated at the top of each chromosome. Scale represents a 5 Mb chromosomal distance

Overexpression of *AeNHL17* enhanced disease resistance in transgenic tobacco and *A. chinensis*

To explore the function of *AeNHL17*, overexpression of *AeNHL17* was performed through the *Agrobacterium*-mediated transformation method in tobacco and kiwifruit, respectively. A specific pair of primers was used to identify positive transgenic plants by using polymerase chain reaction (PCR) analysis (Figs. 7a and 8a). Under normal growth conditions, transgenic tobacco, transgenic kiwifruit, and wild-type (WT) plants did not show obvious phenotypic differences (Supplementary Fig S2).

Three T2 generation plants of transgenic tobacco lines were randomly selected to evaluate whether overexpression of *AeNHL17* could enhance plant resistance to pathogenic bacteria. Over-expression of *AeNHL17* in tobacco was confirmed by semi-quantitative RT-PCR, and the transgenic lines showed higher expression of *AeNHL17* (Fig. 7b). Transgenic and WT tobacco plants were inoculated with Psa and Pst pathogens, respectively. Three days after inoculation, compared to the transgenic lines, the bacterial numbers of both Psa and Pst in the WT increased dramatically (Fig. 7c). Seven days later, the WT leaves turned yellow and displayed necrotic lesions around the inoculation site, whereas the transgenic lines did not show any obvious changes, except for the inoculation wound (Fig. 7d).

Over-expression of *AeNHL17* in kiwifruit was confirmed by semi-quantitative RT-PCR, and the transgenic lines showed GFP fluorescence and higher expression of *AeNHL17* (Fig. 8a-b). For further inoculation tests, the

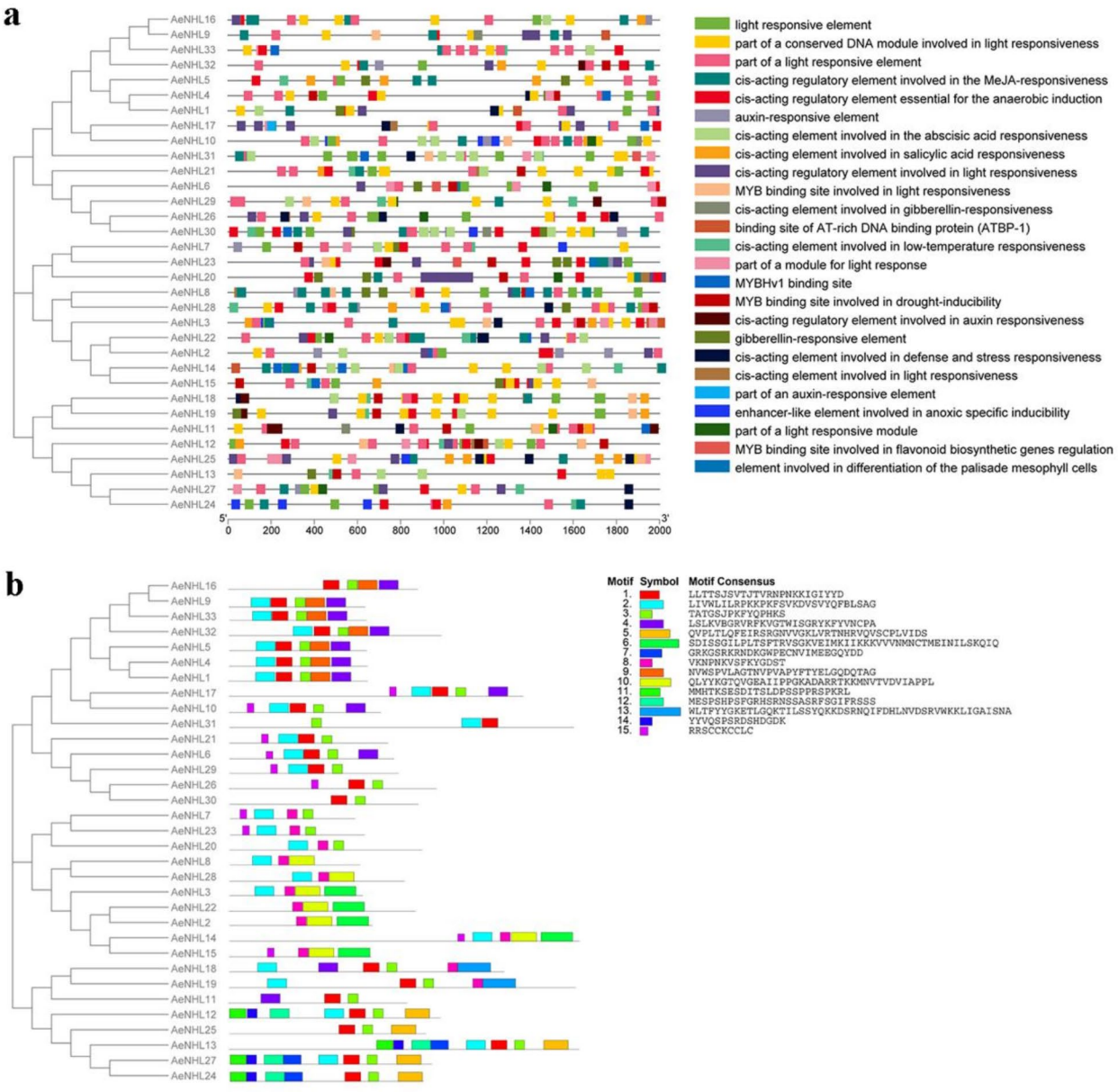

Fig. 3 Schematic representations of the predicted regulatory elements and the conserved motifs in the AeNHL family. **(a)** Schematic illustration of the predicted regulatory elements in the promoter regions of *AeNHLs* by PlantCare. Each regulatory element is marked with a different color. (**b)** Schematic representation of the conserved motifs predicted in the AeNHL proteins. MEME was used to predict the conserved motifs, and TBtools was used to display the results

leaves and stems of both the transgenic and WT lines were inoculated with Psa. The leaves of WT plants turned curly and exhibited yellow disease lesions compared to the transgenic lines at 21 days post-inoculation, whereas the transgenic lines did not show obvious changes, except for the inoculation wound (Fig. 8c). As shown in Fig. 8d, the inoculation area of the WT stem turned brown and the lesion length was as long as 11.83 mm, which was significantly longer than that of the transgenic lines. These results displayed that *AeNHL17*-overexpressed tobacco and kiwifruit plants significantly inhibited pathogen infection, suggesting that the positive function of *AeNHL17* in enhances disease defense.

To further understand the influences of *AeNHL17* in the SA-mediated pathways, the transcription level of some responsive genes was detected in transgenic kiwifruit lines and WT plants, such as pathogenesis-related gene 1 (*PR1*), phytoalexin deficient 4 (*PAD4*), non-expresser of

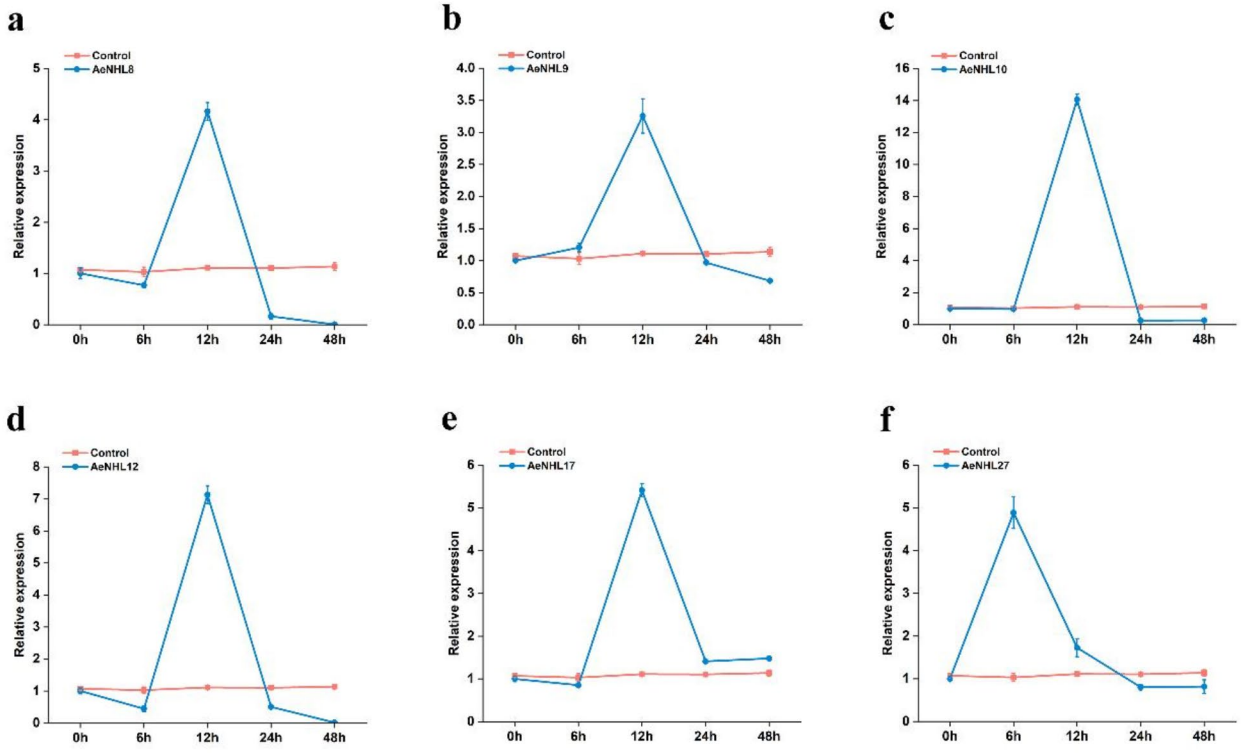

Fig. 4 Relative expression of the *AeNHL8,AeNHL9,AeNHL10,AeNHL12,AeNHL17* and *AeNHL27* genes in kiwifruit leaves after Psa infection. **(a-f)** Expression level of *AeNHL8,AeNHL9,AeNHL10,AeNHL12,AeNHL17* and *AeNHL27* at 6, 12, 24, 48 h after Psa infection. Control indicates plants without Psa infection. The values represent the means ± standard errors (SEs) of three biological replications

pathogenesis-related gene 1 (*NPR1*), isochorismate synthase 1 (*ICS1*), SAR deficient 1 (*SARD1*) and enhanced disease susceptibility 1 (*EDS1*). The results showed that the expression levels of these genes were significantly higher in the transgenic lines than in the WT (Fig. 8e). In summary, we speculated that *AeNHL17* might participate in the disease resistance response by interacting with SA signaling pathways in kiwifruit.

Silencing *AeNHL17* in *A. eriantha* increases susceptibility to Psa

VIGS was utilized to silence *AeNHL17* (TRV::AeNHL17). The transcription level of *AeNHL17* was detected by qPCR analysis at 15 days after infection to evaluate the silencing efficacy of the recombinant plasmid. Compared to the control, the transcription of *AeNHL17*-silenced plants was dramatically reduced (Fig. 9a), demonstrating that the silencing effect of *AeNHL17* was sufficient for subsequent pathogen inoculation experiments. Next, the control and silenced plants were simultaneously inoculated with Psa, and lesion length was measured 21 days after inoculation. Larger disease lesions appeared in the silenced plants than in the control plants (Fig. 9b, c), indicating that silencing *AeNHL17* might increase the susceptibility of *A. eriantha* to Psa.

Identification of proteins interacting with AeNHL17

To further determine the potential proteins that interact with AeNHL17, yeast two-hybrid assays were performed. First, yeast cells co-transformed with pBT3-N-AeNHL17 and pPR3-N showed good growth on DDO, but were not produced on TDO and QDO agar plates (Fig. 10). This revealed that neither the auto-activation of AeNHL17 nor the pBT3-N-AeNHL17 bait plasmid could be used for subsequent library screening.

Eleven AeNHL17-interaction proteins were identified in at least two independent screens (Supplementary Table S3). Based on functional annotations, these proteins were roughly classified into three categories: transport-related proteins, photosynthesis-related proteins and metabolic-related proteins. We selected aldo-keto reductases (AKR), which play important roles in stress defense by eliminating toxic and reactive oxygen species (ROS), as candidate proteins for point-to-point verification. pBT3-N-AeNHL17 co-transformed with pPR3-N-AeAKR grew on DDO, TDO, and QDO medium plates, whereas the negative control did not grow (Fig. 10). These results indicated that AeNHL17 interact with AeAKR.

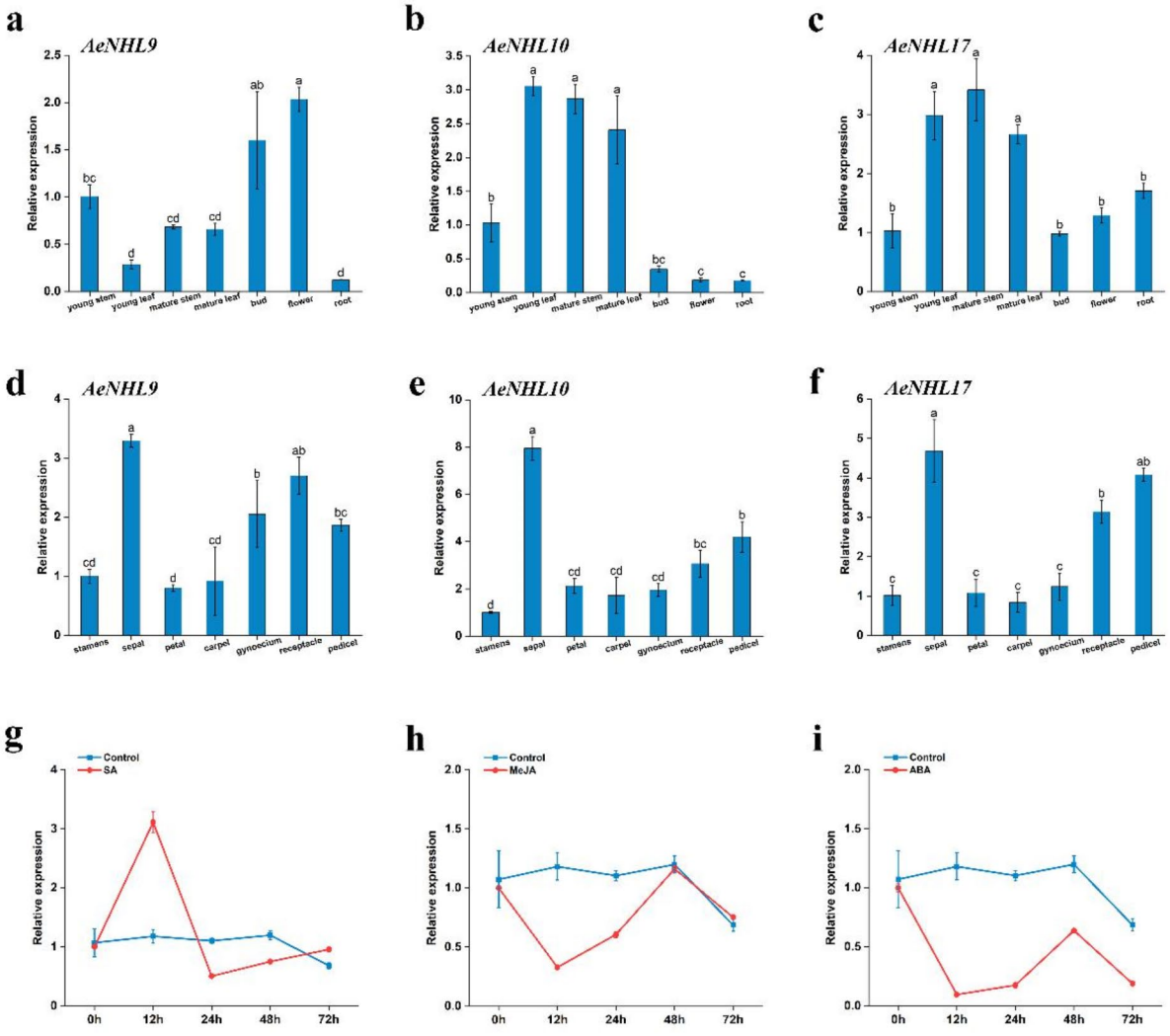

Fig. 5 Expression patterns of *NHL* genes in different tissues and effect of SA, MeJA, and ABA in the expression of *AeNHL17* gene. **(a-f)** Relative expression levels of *AeNHL9*, *AeNHL10* and *AeNHL17* genes in different tissues (young stem, young leaf, mature stem, mature leaf, bud, flower and root) and floral organ (stamens, sepal, petal, carpel, gynoecium, receptacle and pedicel). Data were presented as mean values ± SD ($n = 3$). Lowercase letters in the column denoted the significance level of mean differences at 0.05 (LSD method). **(g-i)** Expression level of *AeNHL17* at 0, 12, 24, 48, 72 h after SA, MeJA, ABA treatments. Control indicates plants without above-mentioned treatments. The values represent the means ± standard errors (SEs) of three biological replications

Discussion

Bacterial cankers have long been a major problem in the kiwifruit industry. Therefore, improving kiwifruit resistance is an effective way to solve this problem. It has been demonstrated that *NHL* gene family is participated in the process of development and disease defense in many plants, such as tobacco, *Arabidopsis*, cotton, grape, and soybean [19, 22, 30–32]. However, there are no reports on *NHL* family members in kiwifruit, particularly their functions in regulating disease resistance. Here, the *NHL* gene family members of kiwifruit were identified, and their protein characteristics and gene expression were analyzed. In addition, we systematically revealed the role of *AeNHL17* in regulating disease resistance.

In the present study, 33 *NHL* family genes in *A. eriantha* were identified (Table 1). Protein sequences analysis, indicated that *AeNHL* gene family members have a conserved LEA domain. Previous studies have documented that proteins with the LEA domain are widely distributed in higher plants and are involved in adjusting plant growth and development, and resisting environmental stresses [23]. LEA-containing proteins in soybean can regulate seed germination under cold stress via the ABA regulation pathway [33]. In tomato, the expression of some *LEA* genes rapidly increases under stress

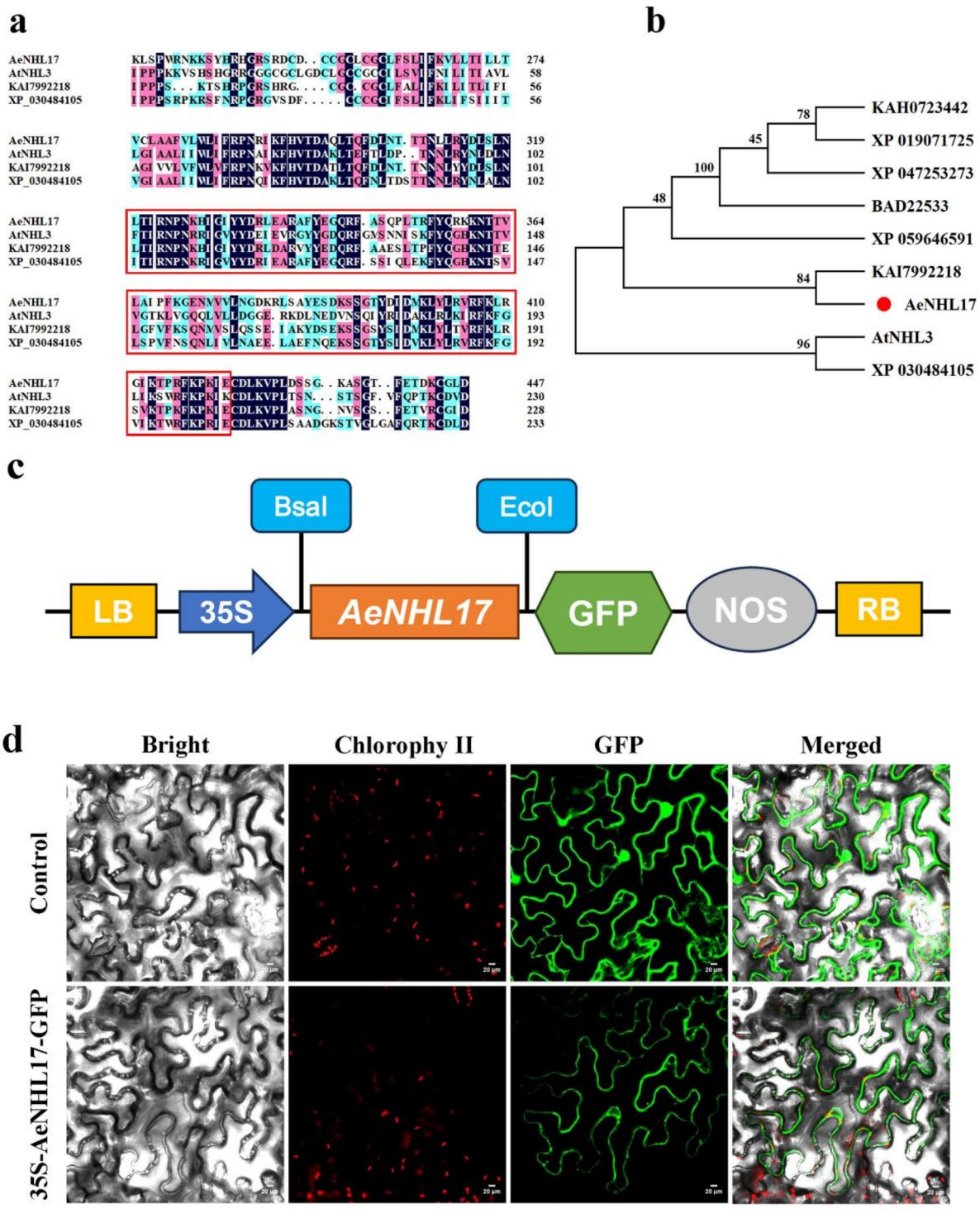

Fig. 6 Multiple sequence alignment, phylogenetic analysis, and subcellular localization of AeNHL17 protein. **(a)** Amino acid sequence alignments of AeNHL17, AtNHL3, KAI7992218 and XP_030484105. The LEA_2 domain was highlighted in red box. **(b)** Phylogenetic tree of AeNHL17 (indicated by a red dot) and other species proteins of *Arabidopsis thaliana* (AtNHL3), *Camellia lanceoleosa* (KAI7992218), *Cornus florida* (XP_059646591), *Capsicum annuum* (XP_047253273), *Cannabis sativa* (XP_030484105), *Solanum tuberosum* (KAH0723442), *Solanum lycopersicum* (XP_019071725) and *Nicotiana tabacum* (BAD22533). **(c)** Schematic representation of 35 S::AeNHL17-GFP fusion construct. **(d)** Subcellular localization of the control (35 S-GFP) and recombinant plasmid (35 S-AeNHL17-GFP) transiently expressed in tobacco leaves and visualized under a confocal microscope. Bar = 20 μm

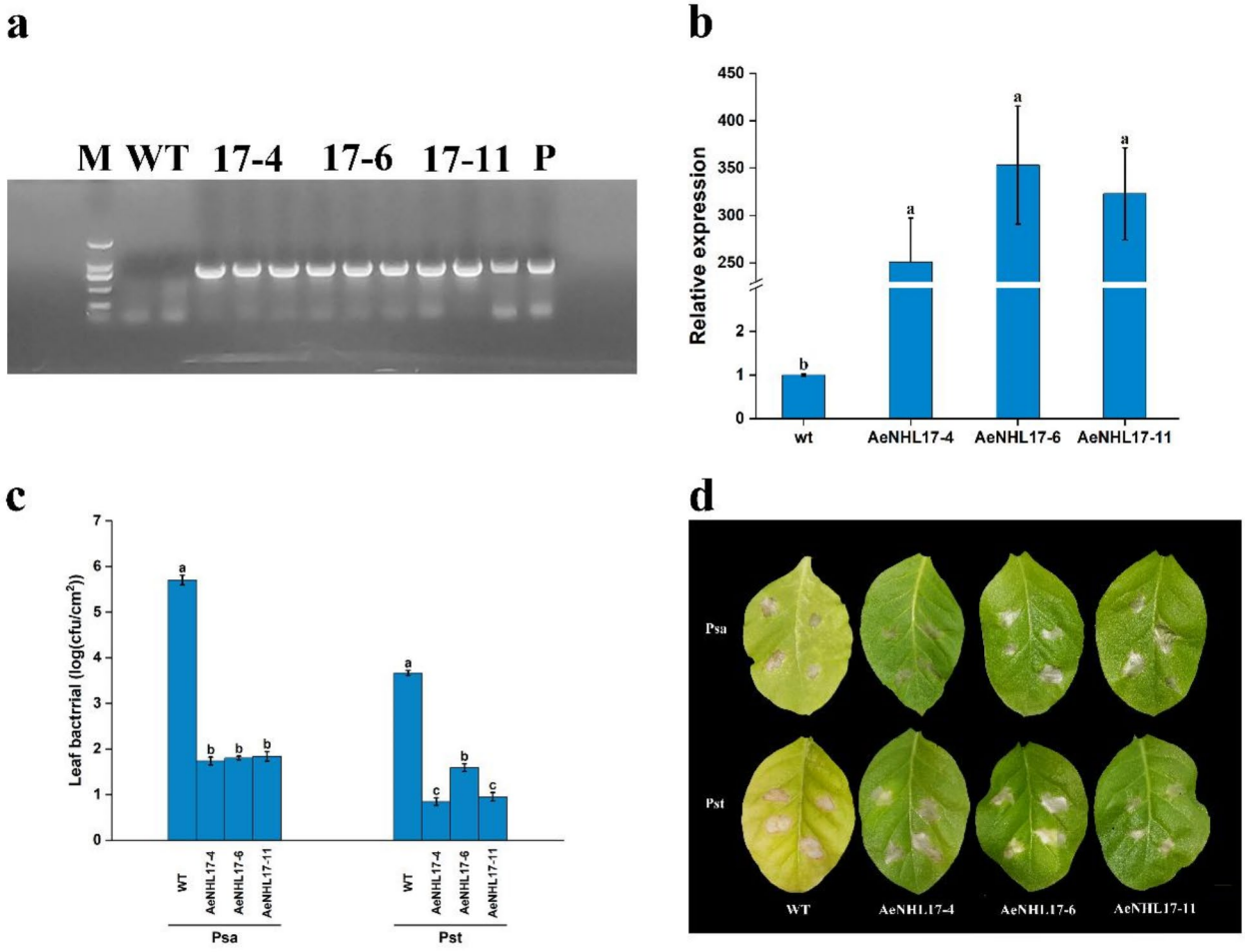

Fig. 7 Overexpression of *AeNHL17* enhances the disease resistance of tobacco. **(a)** Identify positive transgenic plants by using PCR analysis. **(b)** Relative expression of AeNHL17 in WT and transgenic tobacco lines. (**c**) Bacterial growth of *Pseudomonas syringae* pv. *Actinidiae* (Psa) and *Pseudomonas syringae* pv. *Tomato* DC3000 (Pst) in wild-type (WT) and transgenic lines (*AeNHL17-4*, *AeNHL17-6*, *AeNHL17-11*) at 3 days after inoculation. Bacterial growth is expressed as mean values of viable bacteria per square centimeter of leaf tissue. CFU: colony forming unit. (**d**) Disease symptom from representative leaves of WT and transgenic tobacco lines at 7 days after inoculation with Psa and Pst. Data were presented as mean values ± SD ($n = 3$). Lower-case letters in the column denote the significance level of mean differences at 0.05 (LSD method)

and phytohormone treatments [34]. NHLs are a large class of plant defense-related proteins that contain two conserved motifs, NPNKKIGIYYD and PKFYQPHKS, implying that there is also a conserved function between homologous genes [22, 35]. In this study, 15 conserved motifs in 33 AeNHL proteins were identified, which is in accordance with the number of conserved motifs in soybean and pepper [28, 33]. Two highly conserved motifs (1 and 3) were found in *AeNHL* gene family. These results suggest that *NHL* gene family members may be participate in kiwifruit defense resistance.

Phylogenetic analysis revealed that the AeNHL proteins were split into five different subgroups, and homologs with similar domains were divided into the same group, with AeNHL17 being closer to AtNHL3 (Fig. 1). Interestingly, it has been reported that the overexpression *NHL3* in *Arabidopsis* can significantly increase transgenic plant resistance to virulent *Pseudomonas syringae* [36], indicating that *AeNHL17* play a vital role in defense resistance in kiwifruit.

Plant hormones such as SA, ABA, GA, and MeJA play critical roles in the response to biotic and abiotic stresses, which are controlled by cis-acting regulatory elements [37]. Cis-element analysis indicated that the promoter region of *AeNHLs* included numerous stress- and defense-related elements and hormone induction elements (Fig. 3a), indicating that members of *AeNHL* gene family might be involved in the kiwifruit resistance response. Most studies have demonstrated that *NHLs* involve in the SA-mediated defense response pathway and other stress response [26, 38]. In kiwifruit, *AeNHL25* contained four SA-responsive elements, and

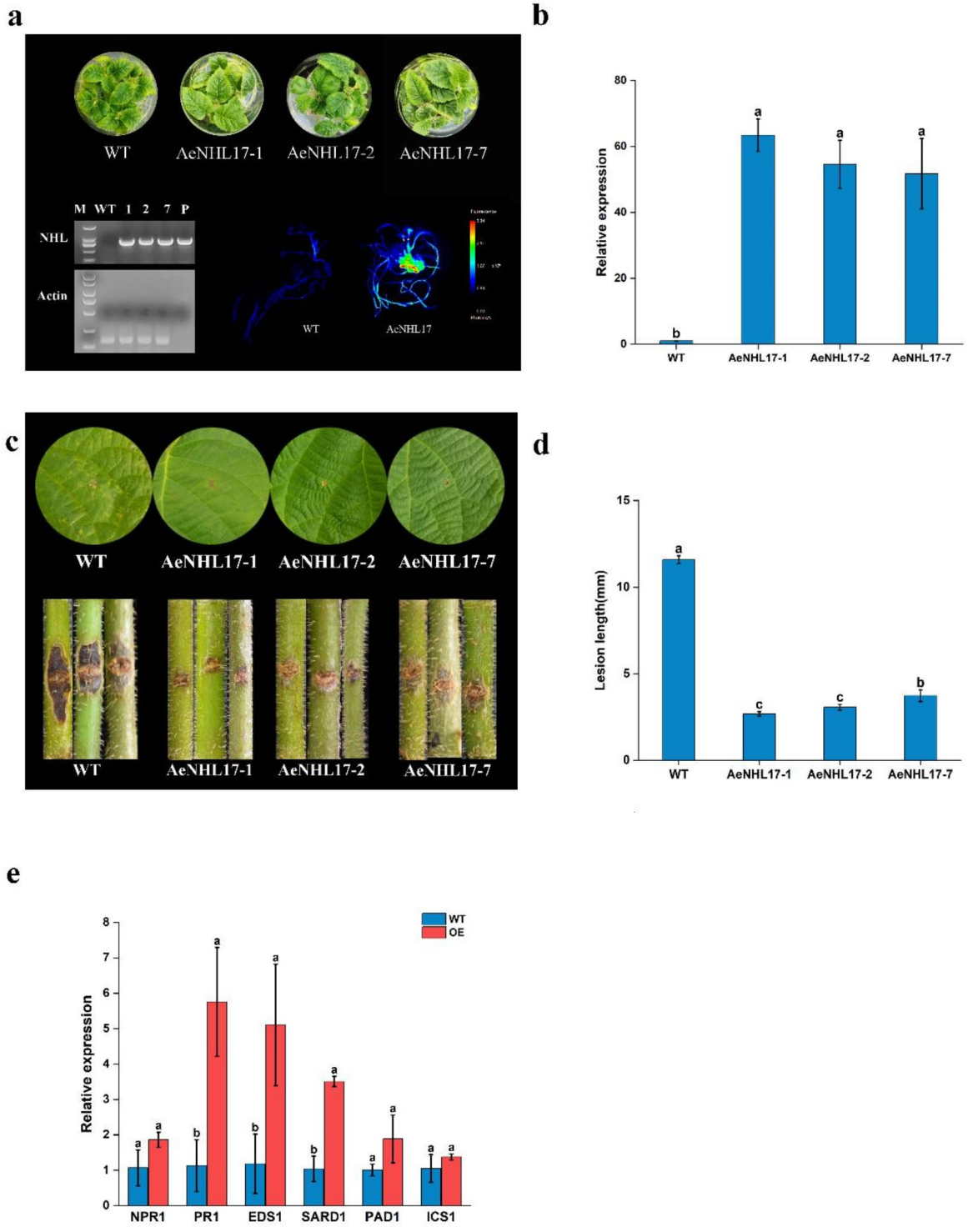

Fig. 8 Overexpression of *AeNHL17* enhances the disease resistance of kiwifruit plants. **(a)** PCR and fluorescence image for identification of positive transgenic kiwifruit plants based on the expression GFP reporter genes. (**b)** Relative expression of *AeNHL17* in WT and transgenic kiwifruit lines. (**c)** Disease symptom of leaves and stems in WT and transgenic kiwifruit lines at 21 days after inoculation with Psa. (**d)** Lesion length of stems in WT and transgenic kiwifruit lines at 21 days after inoculation with Psa. (**e)** Effects of overexpression of *AeNHL17* on the expression of the SA-responsive genes *NPR1*, *PR1*, *EDS1*, *SARD1*, *PAD1* and *ICS1* in transgenic lines and WT. The all results are presented from three independent experiments. Data were presented as mean values ± SD ($n = 3$). Lower-case letters in the column denote the significance level of mean differences at 0.05 (LSD method)

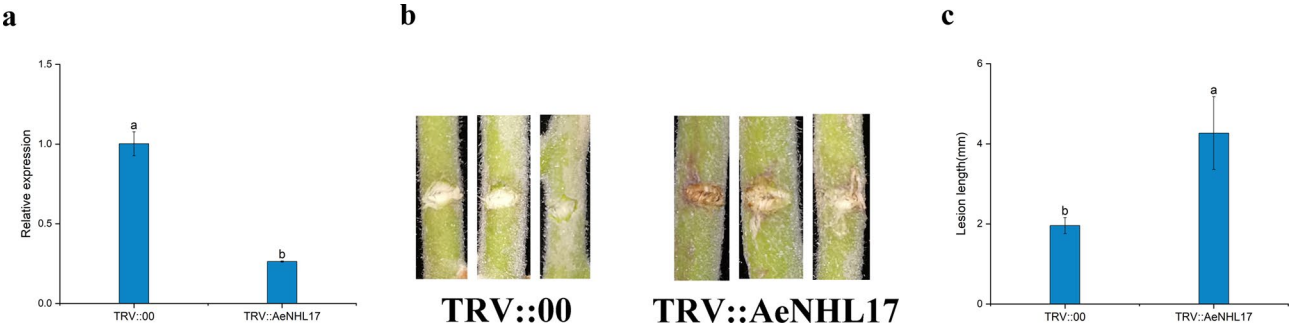

Fig. 9 Silencing *AeNHL17* in *A. eriantha* increases susceptibility to Psa. **(a)** The expression level of *AeNHL17* was quantified by qPCR at 15 days after inoculation with TRV1 + TRV::AeNHL17 and TRV1 + TRV::00, respectively. (**b-c)** Silencing *AeNHL17* increases infection of Psa. Disease symptom of stems and lesion length was measured at 21 days after inoculation. The values represent means ± standard errors (SEs) of three biological replications. The lower-case letters in the column denote the significance level of mean differences at 0.05

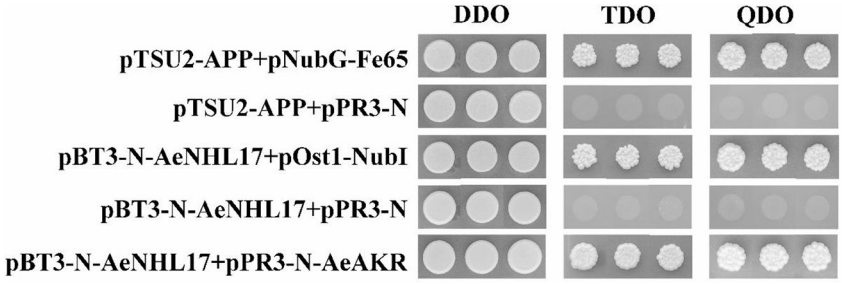

Fig. 10 Yeast two-hybrid assays of AeNHL17 protein. The pBT3-N-AeNHL17 and pOST1-NubI, pPR3-N were co-transformed into yeast NMY51 strains and cultured on DDO, TDO, QDO agar plates, respectively. The CDS of *AeAKR* was cloned into the prey vector pPR3-N and co-transformed with the bait vector pBT3-N-AeNHL17. Yeast cells co-transformed with pTSU2-App and pNubG-Fe65, pTSU2-App and pPR3-N were used as positive and negative controls, respectively

other members including *AeNHL3*, *AeNHL5*, *AeNHL10*, *AeNHL11*, *AeNHL12*, *AeNHL14*, *AeNHL15*, *AeNHL16*, *AeNHL18*, *AeNHL19*, *AeNHL21*, *AeNHL24*, *AeNHL28* and *AeNHL32*, also contain SA-responsive elements (Fig. 3a). These results indicate that *AeNHL* genes may play a positive role in disease defense by being involved in the SA-induced pathway. The results of qPCR analysis indicated that *AeNHL17* was strongly triggered after treatment with exogenous SA (Fig. 5g). However, the promoter of *AeNHL17* lacks the cis-acting elements of SA, suggesting that *AeNHL17* may not be directly involved in the SA signaling pathway. In addition, the experimental results showed that the expression of the SA signaling pathway genes *NPR1*, *ICS1*,*PAD4*, *EDS1*, *PR1*, and *SARD1* increased in *AeNHL17* transgenic plants, indicating that overexpression of *AeNHL17* in kiwifruit might improve the transcription level of the SA pathway genes. The promoter region of *AeNHL17* contained ABA- and JA-responsive elements (Fig. 3a). However, the expression of *AeNHL17* decreased with JA and ABA treatments (Fig. 5h-i). The results indicated that ABA and JA might have negative regulatory roles in Psa infection, and these results were consistent with those of a previous study [39]. Therefore, we speculated that the different expression patterns of individual *AeNHL* genes led to differences in response to exogenous hormone treatment in this study, and the predicted regulatory elements in the promoter regions were not strongly correlated with the activated expression of particular genes.

The plasma membrane is very important for pathogen signal recognition or downstream defense signal generation [36, 40]. It has been documented that NHL proteins are localized on the plasma membrane [41]. Similarly, our results indicated that AeNHL17 was mainly localized on the plasma membrane (Fig. 6d); therefore, we hypothesized that AeNHL17 might also participate in pathogen perception and the rapid induction of defense responses. The results showed that *AeNHL17* was highly induced by Psa infection (Fig. 4e). Overexpression of *NHL3* enhances the resistance of *Arabidopsis* to *Pseudomonas syringae* pv. *tomato* DC3000 [36]. Transgenic tobacco and kiwifruit showed that the disease symptoms were significantly lower after *P. syringae* infection than in WT plants (Figs. 7b and 8c). In contrast, silencing *AeNHL17* in kiwifruit increased susceptibility to Psa (Fig. 9b-c). The overexpression lines showed enhanced resistance, and no significant morphological or phenotypic changes were observed in the transgenic plants. Taken together, these findings indicate that *AeNHL17* participates in the rapid disease resistance of plants during pathogen infection.

Under biotic and abiotic stress conditions, the expression of reactive oxygen species (ROS) increases significantly, leading to lipid peroxidation, which produces toxic compounds such as 4-hydrocynonenal (4-HNE) and malondialdehyde (MDA), causing cell damage [42, 43]. Aldo-keto reductases (AKR) are a superfamily of oxidoreductases that can reduce aldehydes and ketones to alcohol [44]. It has been reported that *AKR1* could effectively eliminate toxic 4-HNE and MDA compounds and enhances stress resistance in rice [45]. Overexpression of *PsAKR1* reduced the levels of methylglyoxal (MG), H_2O_2, and MDA, and improved chlorophyll content and plant survival under salt stress [43]. In our study, the interaction between AeNHL17 and AeAKR suggests that AKR might improve chlorophyll content and enhance membrane stability in kiwifruit under pathogenic attack. In transgenic kiwifruits, the interaction between AeNHL17 and AeAKR may enhances the ability of cells to eliminate toxic 4-HNE and MDA compounds in Psa infection. However, further research is required to elucidate the precise mechanisms underlying AKR in kiwifruit.

Conclusion

Here, we identified 33 potential *NHL* family members in *A. eriantha* for the first time using a genome-wide method, and then classified and analyzed these genes. We found that *AeNHL17* plays an important role in kiwifruit disease defense. Functional analysis indicated that overexpression of *AeNHL17* in kiwifruit and tobacco bestows transgenic plants with resistance to pathogens, based on the noticeable differences in disease lesion symptoms between transgenic and WT lines. Based on these results, we propose that the enhanced resistance of kiwifruit may be caused by a complex interaction involving AeNHL17, AeAKR and defense genes related to the SA signaling pathway (Fig. 11). Further functional analyses of the kiwifruit *NHL* genes are required to enhance our understanding of their biological roles. Our findings will contribute to the genetic improvement of kiwifruit and the development of more resistance resources.

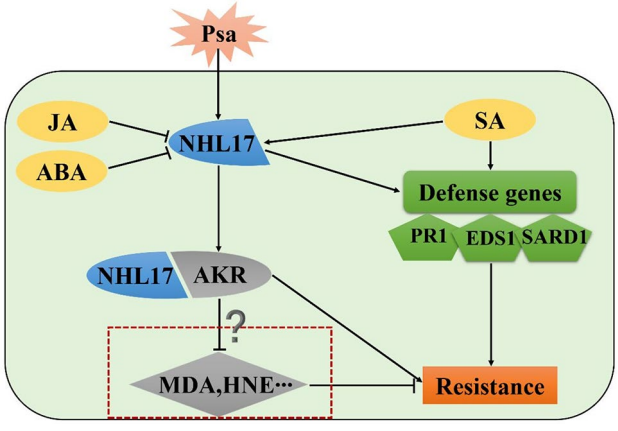

Fig. 11 The schematic diagram of the mechanism by which overexpressed *AeNHL17* enhanced the resistance of kiwifruit under Psa attacked. Both Psa and SA could induce the expression of AeNHL17, while JA and ABA exhibit negative regulatory effects. AeNHL17 interacts with AeAKR protein and AKR could eliminate MAD and HNE. In parallel, overexpression of AeNHL17 could enhance the accumulation of resistance genes expression in the SA pathway. They work together to improve the disease resistance of transgenic kiwifruit

Materials and methods

Plant materials and bacterial stains

The kiwifruit materials Zhongmi Cuixue 1 Hao (*Actinidia eriantha*), 'Hongyang' (*Actinidia chinensis*), and tobacco NC89 (*Nicotiana tabacum*) were grown in soil (perlite: vermiculite=1:1). Kiwifruit plants were grown for 4 months and NC89 for 4 weeks at the artificial climate chamber under a 75% relative humidity, 25℃ temperature and 12 h/12 h light/dark.

Agrobacterium tumefaciens GV3101 and EHA105 were cultured in liquid LB medium with 25 mg/ml rifampicin (rif) and 50 mg/ml kanamycin (kan) for 2 d at 200 rpm 28℃ in an orbital shaker. After two days, the bacterial medium was resuspended in MS (pH 5.8) at the desired concentrations for infiltration.

Pseudomonas syringae pv. *tomato* DC3000 (Pst) and *Pseudomonas syringae* pv. *actinidiae* (Psa) was grown in KB medium supplemented for 1d at 23℃ in an orbital shaker at 150 rpm. After 24 h, bacterial cultures were resuspended in 10 mM magnesium chloride ($MgCl_2$) for infiltration.

Genome-wide identification of NHL genes

To identify the members of Ae*NHLs*, genome-wide sequences files of *A. eriantha* 'White' were downloaded from the Kiwifruit Genome Database (KGD) (https://kiwifruitgenome.org/) [46, 47]. 45 *Arabidopsis NHL* gene family sequences were downloaded from the TAIR database (https://www.arabidopsis.org/). By using the BLASTp program, we settled the candidate sequence with $E \leq e^{-10}$. The theoretical isoelectric point (pI) and molecular weight (MW) were calculated using ProtParam website (https://web.expasy.org/protparam/). And Hidden Markov models (HMMs) from the SMART database (http://smart.embl.de/) were used to predict protein domain structures [48]. These protein sequences, including the LEA-2 conserved domain, were regarded as *AeNHL* genes of *A. eriantha*.

Phylogenetic analysis and chromosomal localization

Multiple sequence alignments (MAS) of AeNHL proteins were performed, and an unrooted phylogenetic tree was constructed using MEGA 11.0.13 software with the neighbor-joining (NJ) method [49]. Bootstrap replications were set to 1000. The chromosome location

information of *AeNHLs* was extracted based on positional information from KGD [47]. All *AeNHL* genes were mapped to their respective loci in the kiwifruit genome and visualized using TBtools software [50].

Conserved motif and cis-element enrichment analysis

To determine the conserved motifs in the 33 AeNHL protein sequences, the online Multiple Em for Motif Elicitation (MEME) tool was used [51] (https://meme-suite.org/meme/tools/meme). The optimization parameter settings were as follows: maximum number of motifs, 15; site distribution, zero or one occurrence per sequence; and optimum width of each motif, between 6 and 50 residues. The motif structure was displayed using TBtools [50].

To explore the regulatory elements of *AeNHL* genes, a 2000 bp upstream sequence of the start codon (ATG) was extracted from the whole genome files using TBtools, and the sequences were run through the online PlantCare website (http://bioinformatics.psb.ugent.be/webtools/plantcare/html/). The regulatory element structure was shown by TBtools [50, 52].

Expression analysis of *AeNHLs*

Quantitative real-time RT-PCR was performed to examine the expression patterns of some members of *AeNHL* family in various tissues and floral organs. Total RNAs were extracted using an RNA Extraction Kit (Vazyme, China), and the first-strand cDNAs were synthesized using reverse transcriptase (ReverTra, TOYOBO) following the manufacturer's instructions.

qRT-PCR was performed using the NovoStart SYBR qPCR SuperMix Plus Kit (Novoprotein, China) on a Roche Light 480 System (Roche, USA) to evaluate the transcript levels of *AeNHL* family members. The Primer premier 5.0 tool was used to design primers based on the CDS of each gene (Supplementary Table S1). The relative changes in gene transcription levels were calculated using the $2^{-\Delta\Delta CT}$ method, and the kiwifruit actin was used as the internal reference gene to normalize the results. All analysis were performed using four technical replicates and three biological replicates.

Cloning of the *AeNHL17* cDNA

To clone the full-length cDNA of *AeNHL17*, specific-primers were designed based on the open-reading frame (ORF) of the *A. eriantha* gene DTZ71_15g07880 (Supplementary Table S1). The PCR products were purified using a GeneJET Gel Extraction Kit (Thermo Scientific, Germany) and cloned into the pCE2 TA/Blunt-Zero Cloning vector (Vazyme, China) for sequencing. A minimum four clones were sequenced.

The MW and pI of AeNHL17 were predicted using the ExPASy tool (https://web.expasy.org/protparam/). The homologous proteins from other species of AeNHL17 were retrieved from the TIAR website and NCBI database. The MEGA 11.0.13 software was used to construct an unrooted phylogenetic tree, and the DNAMAN (v9.0.1.116) tool was used to determine the MSA for AeNHL17 and other homologous proteins.

Subcellular localization of AeNHL17 protein

For subcellular localization, the ORF sequence without the stop codon of *AeNHL17* was inserted into a pBWA(V)HS-GFP vector using the restriction sites *Bsa*I and *Eco*RI. Plasmids harboring GFP alone were used as controls. These recombinant plasmids were transformed into tobacco leaves by infiltration with *A. tumefaciens* GV3101. A laser confocal microscope was used to observe the GFP green fluorescence signals.

Exogenous hormones and pathogen treatment

To investigate the effects of exogenous hormones on *AeNHL17* expression, the *A. eriantha* grafted plants were treated with 5 mmol/L SA (Sigma, USA), 50 μmol/L ABA (Sigma, USA), or 0.1 mmol/L MeJA (Sigma, USA) at three months after grafting, respectively. The mock plants were treated with sterile water.

For *Psa* inoculation, an overnight fresh bacterial culture was adjusted to a final concentration of 1×10^8 cfu/L with sterile 10 mM $MgCl_2$ (Sigma, USA) solution, and then sprayed onto the kiwifruit leaves. Each experiment was conducted in triplicates replicates, using at least three independent plants. All samples were collected at 0, 12, 24, 48, and 72 h, were frozen in liquid nitrogen immediately and stored at -80℃ for RNA isolation.

Overexpression and VIGS vectors construction

To construct a vector for the overexpression of *AeNHL17*, the restriction sites of *Xba*I and *Bam*HI were introduced into the full-length cDNA of *AeNHL17*, and the fragment was cloned into the pBI121-GFP vector. For virus-induced gene silencing (VIGS), an *XbaI- BamHI* fragment containing 300 bp of *AeNHL17* was cloned into a pTRV2 vector. All expression vector primers used throughout the experiment are provided in the Supporting Information.

Agrobacterium-mediated transformation

The vector pBI121-*AeNHL17*-GFP was transformed into *A. tumefaciens* strains EHA105 and GV3101, respectively. Tobacco genetic transformation was performed according to a previously reported *Agrobacterium*-mediated transformation method using GV3101 [53], and transformation of kiwifruit (*A. chinensis* cv. Hongyang) was performed using EHA105 based on the instructions reported by Wang [54]. The DNA of the wild-type (WT) and transgenic plants was extracted using a plant genomic DNA kit (TIANGEN, China), and positive

transgenic plants were confirmed by PCR amplification using the primers 35 S-F and AeNHL17-R (Supplementary Table S1).

For the kiwifruit VIGS assays, pTRV1 was used along with pTRV2 for silencing. *Agrobacterium* GV3101 with pTRV1, pTRV2 empty vector or pTRV2-AeNHL17 vector was resuspended in induction medium (10 μm MES, 10 μm MgCl2, 400μ macetosyringone) and diluted to OD600 0.7, followed by incubating for 3 h at room temperature. The diluted cultures containing pTRV1 and pTRV2-AeNHL17 were then mixed in a 1:1 ratio, and a mixture of pTRV1 and pTRV2 was used as a mock control. The mixed culture was then infiltrated into the stems of *A. eriantha* plants.

Measurement of pathogen resistance in transgenic plants

To determine the disease resistance of *AeNHL17* transgenic lines, the plants were inoculated with both Psa and Pst pathogens according to a previously described protocol with a few modifications [39, 55]. The strains were resuspended at 1×10^8 cfu/L in sterile 10 mM $MgCl_2$ solution. Leaves of 5-week-old transgenic and non-transgenic tobacco plants were inoculated with Psa and Pst. Kiwifruit infection was carried out in 6-month-old transgenic and WT plants by leaf spraying and stem inoculation with Psa. Three days after inoculation, the tobacco leaves were collected from the treated plants, washed with sterile water, and ground with sterile $MgCl_2$ (10 mM). The suspensions were serially diluted and plated onto KB agar plates. The number of CFU per disk leaf was calculated after 3 days incubation at 23℃. Phenotypic changes in tobacco were observed continuously after infection and photographed on the seventh day. Leaf and stem lesion sizes of kiwifruit were monitored and measured 21 days post-inoculation.

Yeast two-hybrid assays

For Y2H assays, the DUALmembrane system (Clontech, USA) was used to screen proteins interacting with AeNHL17, following a previously described protocol [56, 57]. The amplified full-length CDS of AeNHL17 was digested with SfiI enzyme and cloned into the pBT3-N vector to construct the bait. To evaluate whether pBT3-N-AeNHL17 exhibited self-activation and toxicity, pBT3-N-AeNHL17 was co-transformed with pPR3-N and pOST1-NubI respectively. The interaction between pTSU2-App and pNubG-Fe65 was used as the positive control, whereas pTSU2-App and pPR3-N were used as negative controls. They spotted onto SD/-Trp/-Leu (double dropout supplement, DDO), SD/-Trp/-Leu/-His (triple dropout supplement, TDO) and SD/-Trp/-Leu/-His/-Ade (quadruple dropout supplement, QDO) solid mediums. For library screening, the expression vector pBT3-N-AeNHL17 and library plasmids were co-transformed and plated on QDO solid mediums. pBT3-N-AeNHL17 was co-transformed with the reciprocal protein and spotted onto DDO, TDO and QDO plates for point-to-point validation. The yeast NMY51 strain was used. The primers used for Y2H are listed in Supplementary Table S1.

Statistical analysis

At least three replicates of the experiments and data were used in this study. For statistical analysis, the Software OriginPro 2023 (OriginLab Corporation, USA) was used to calculate the means and standard deviations of all data. The Dunn-Sidak test was performed to evaluate the significance level with $P<0.05$ or $P<0.01$.

Supplementary Information

The online version contains supplementary material available at https://doi.org/10.1186/s12870-024-05936-2.

Supplementary Material 1

Supplementary Material 2

Supplementary Material 3

Supplementary Material 4

Supplementary Material 5

Acknowledgements

Not applicable.

Author contributions

L.S. and X.Q. designed and supervised this project. M.Z. carried out the majority of the experiments. R.F. and M.L. performed expression analysis and data collection. R.W. and Y.L. assisted with the analysis of the results. L.S., X.Q., J.F. and J.C. provided guidance on the study. M.Z. and L.S. wrote the manuscript. All the authors reviewed and approved the ultimate manuscript.

Funding

This work was financially supported by the Major Science and Technology Projects of Henan Province (221100110400), National Key Research and Development Program (2022YFD1600700), China Agriculture Research System of MOF and MARA (CARS-26), Agricultural Science and Technology Innovation Program of the Chinese Academy of Agricultural Sciences (CAAS-ASTIP-2024-ZFRI-03), and Henan Agriculture Research System (HARS-22-09-S).

Data availability

All the experimental data are included in the main text and the supplementary data.

Declarations

Ethics approval and consent to participate

Not applicable.

Consent for publication

Not applicable.

Competing interests

The authors declare no competing interests.

Received: 5 September 2024 / Accepted: 4 December 2024
Published online: 18 December 2024

References

1. Sui L, Liu Y, Zhong C, Huang H. Geographical distribution and morphological diversity of red-fleshed kiwifruit germplasm (*Actinidia chinensis* Planchon) in China. Genet Resour Crop Ev. 2013;60(6):1873–83.
2. Huang S, Ding J, Deng D, Tang W, Sun H, Liu D, Zhang L, Niu X, Zhang X, Meng M, Yu J, Liu J, Han Y, Shi W, Zhang D, Cao S, Wei Z, Cui Y, Xia Y, Zeng H, Bao K, Lin L, Min Y, Zhang H, Miao M, Tang X, Zhu Y, Sui Y, Li G, Sun H, Yue J, Sun J, Liu F, Zhou L, Lei L, Zheng X, Liu M, Huang L, Song J, Xu C, Li J, Ye K, Zhong S, Lu B-R, He G, Xiao F, Wang H-L, Zheng H, Fei Z, Liu Y. Draft genome of the kiwifruit *Actinidia chinensis*. Nat Commun. 2013;4(1):2640.
3. Mazzaglia A, Studholme DJ, Taratufolo MC, Cai RM, Almeida NF, Goodman T, Guttman DS, Vinatzer BA, Balestra GM. *Pseudomonas syringae* Pv. *Actinidiae* (PSA) isolates from recent bacterial canker of kiwifruit outbreaks belong to the same genetic lineage. PLoS ONE 2012, 7(5).
4. Vanneste JL. The scientific, economic, and social impacts of the New Zealand outbreak of bacterial canker of kiwifruit (*Pseudomonas syringae* Pv. *Actinidiae*). Annu Rev Phytopathol 2017: 377–99.
5. McCann HC, Li L, Liu Y, Li D, Pan H, Zhong C, Rikkerink EHA, Templeton MD, Straub C, Colombi E, Rainey PB, Huang H. Origin and evolution of the kiwifruit canker pandemic. Genome Biol Evol. 2017;9(4):932–44.
6. Scortichini M. Occurrence of *Pseudomonas syringae* Pv. *Actinidiae* on kiwifruit in Italy. Plant Pathol. 1994;43:1035–8.
7. Koh Y, Kim G, Jung J, Lee Y, Hur J. Outbreak of bacterial canker on Hort16A (*Actinidia chinensis* Planchon) caused by *Pseudomonas syringae* Pv. Actinidiae Korea New Zeal J Crop Hort. 2010;38:275–82.
8. Scortichini M, Marcelletti S, Ferrante P, Petriccione M, Firrao G. *Pseudomonas syrPvgae* pv. *actinidiae*: a re-emerging, multi-faceted, pandemic pathogen. Mol Plant Pathol. 2012;13(7):631–40.
9. Serizawa S, Ichikawa T, Takikawa Y, Tsuyumu S, Goto M. Occurrence of bacterial canker of kiwifruit in Japan description of symptoms, isolation of the pathogen and screening of bactericides. Japanese J Phytopathol. 1989;55(4):427–36.
10. Sawada H, Fujikawa T. Genetic diversity of *Pseudomonas syringae* Pv. *Actinidiae*, pathogen of kiwifruit bacterial canker. Plant Pathol. 2019;68(7):1235–48.
11. McCann HC, Rikkerink EHA, Bertels F, Fiers M, Lu A, Rees-George J, Andersen MT, Gleave AP, Haubold B, Wohlers MW, Guttman DS, Wang PW, Straub C, Vanneste J, Rainey PB, Templeton MD. Genomic analysis of the kiwifruit pathogen *Pseudomonas syringae* pv. *actinidiae* provides insight into the origins of an emergent plant disease. Plos Pathog. 2013, 9(7).
12. Donati I, Cellini A, Sangiorgio D, Vanneste JL, Scortichini M, Balestra GM, Spinelli F. *Pseudomonas syringae* pv. *actinidiae*: ecology, infection dynamics and disease epidemiology. Microb Ecol 2020, 80(1):81–102.
13. Kinkema M, Fan WH, Dong XN. Nuclear localization of *NPR1* is required for activation of *PR* gene expression. Plant Cell. 2000;12(12):2339–50.
14. Jones J, Dangl J. The plant immune system. Nature. 2006;444(7117):323–9.
15. Balint-Kurti P. The plant hypersensitive response: concepts, control and consequences. Mol Plant Pathol. 2019;20(8):1163–78.
16. Shi H, Shen Q, Qi Y, Yan H, Nie H, Chen Y, Zhao T, Katagiri F, Tang D. BR-SIGNALING KINASE1 physically associates with FLAGELLIN SENSING2 and regulates plant innate immunity in *Arabidopsis*. Plant Cell. 2013;25(3):1143–57.
17. Yalpani N, Silverman P, Wilson TM, Kleier DA, Raskin I. Salicylic acid is a systemic signal and an inducer of pathogenesis-related proteins in virus-infected tobacco. Plant Cell 1991, 3(8):809–18.
18. Vlot AC, Dempsey DMA, Klessig DF. Salicylic acid, a multifaceted hormone to combat disease. Annu Rev Phytopathol. 2009;47(1):177–206.
19. Takahashi Y, Berberich T, Yamashita K, Uehara Y, Miyazaki A, Kusano T. Identification of tobacco *HIN1* and two closely related genes as spermine-responsive genes and their differential expression during the tobacco mosaic virus-induced hypersensitive response and during leaf- and flower-senescence. Plant Mol Biol. 2004;54(4):613–22.
20. Century KS, Shapiro AD, Repetti PP, Dahlbeck D, Holub E, Staskawicz BJ. *NDR1*, a pathogen-induced component required for *Arabidopsis* disease resistance. Science. 1997;278(5345):1963–5.
21. Peng H, Pu Y, Yang X, Wu G, Qing L, Ma L, Sun X. Overexpression of a pathogenesis-related gene *NbHIN1* confers resistance to tobacco mosaic virus in *Nicotiana benthamiana* by potentially activating the jasmonic acid signaling pathway. Plant Sci. 2019;283:147–56.
22. Dormann P, Gopalan S, He SY, Benning C. A gene family in *Arabidopsis* thaliana with sequence similarity to *NDR1* and *HIN1*. Plant Physiol and Bioch 2000, 38(10):789–96.
23. Hong BS, Zong SL, Ming AS. LEA proteins in higher plants: structure, function, gene expression and regulation. Colloids Surf B. 2005;45(3):131–5.
24. Shapiro AD, Zhang C. The role of *NDR1* in avirulence gene-directed signaling and control of programmed cell death in *Arabidopsis*. Plant Physiol. 2001;127(3):1089–101.
25. Varet A, Parker J, Tornero P, Nass N, Lee J. *NHL25* and *NHL3*, two NDR1/HIN1-1ike genes in *Arabidopsis thaliana* with potential role(s) in plant defense. Mol Plant Microbe in. 2002;15(6):608–16.
26. Zheng MS, Takahashi H, Miyazaki A, Hamamoto H, Shah J, Yamaguchi I, Kusano T. Up-regulation of *Arabidopsis thaliana NHL10* in the hypersensitive response to cucumber mosaic virus infection and in senescing leaves is controlled by signalling pathways that differ in salicylate involvement. Planta. 2004, 218(5):740–750.
27. Chen Q, Tian Z, Jiang R, Zheng X, Xie C, Liu J. *StPOTHR1*, a NDR1/HIN1-like gene in *Solanum tuberosum*, enhances resistance against Phytophthora infestans. Biochem Bioph Res Co. 2018;496(4):1155–61.
28. Liu C, Peang H, Li X, Liu C, Lv X, Wei X, Zou A, Zhang J, Fan G, Ma G, Ma L, Sun X. Genome-wide analysis of NDR1/HIN1-like genes in pepper (*Capsicum annuum* L.) and functional characterization of *CaNHL4* under biotic and abiotic stresses. Hortic Res. 2020;7:93.
29. Letunic I, Bork P. Interactive tree of life (iTOL) v6: recent updates to the phylogenetic tree display and annotation tool. Nucleic Acids Res; 2024.
30. Chong J, Le Henanff G, Bertsch C, Walter B. Identification, expression analysis and characterization of defense and signaling genes in *Vitis vinifera*. Plant Physiol Bioch. 2008;46(4):469–81.
31. Zhang X, Xue Y, Wang H, Nisa ZU, Jin X, Yu L, Liu X, Yu Y, Chen C. Genome-wide identification and characterization of *NHL* gene family in response to alkaline stress, ABA and MEJA treatments in wild soybean (*Glycine soja*). PeerJ. 2022;10:e14451.
32. Guo XH, Wei F, Jian HL, Lian BY, Dang XY, Yang MQ, Fu XK, Ma L, Lu JH, Wang HT, Wei HL, Yu SX. Systematic analysis of the NDR1/HIN1-like (*NHL*) family in *Gossypium hirsutum* reveals a role of *GhNHL69* in responding to cold stress. Industrial Crops and Products 2023, 206.
33. Wang J, Wu R, Shangguan T, Chen G, Zheng Y, Tao X, Li S, Wang Y, Xu S. NDR1/HIN1-like genes may regulate Glycine max seed germination under chilling stress through the ABA pathway. Plant Growth Regul. 2022;98(3):613–24.
34. Jia C, Guo B, Wang B, Li X, Yang T, Li N, Wang J, Yu Q. The *LEA* gene family in tomato and its wild relatives: genome-wide identification, structural characterization, expression profiling, and role of *SlLEA6* in drought stress. BMC Plant Biol. 2022;22(1):596.
35. Hu L, Liu S. Genome-wide identification and phylogenetic analysis of the *ERF* gene family in cucumbers. Genet Mol Biol. 2011;34(4):624–33.
36. Varet A, Hause B, Hause G, Scheel D, Lee J. The *Arabidopsis NHL3* gene encodes a plasma membrane protein and its overexpression correlates with increased resistance to *Pseudomonas syringae* Pv. *Tomato* DC3000. Plant Physiol. 2003;132(4):2023–33.
37. Ku YS, Sintaha M, Cheung MY, Lam HM. Plant hormone signaling crosstalks between biotic and abiotic stress responses. Int J Mol Sci 2018, 19(10).
38. Bao Y, Song WM, Zhang HX. Role of *Arabidopsis NHL* family in ABA and stress response. Plant Signal Behav. 2016;11(5):e1180493.
39. Song Y, Sun L, Lin M, Chen J, Qi X, Hu C, Fang J. Comparative transcriptome analysis of resistant and susceptible kiwifruits in response to *Pseudomonas syringae* Pv. *Actinidiae* during early infection. PLoS ONE. 2019;14(2):e0211913.
40. Knepper C, Savory EA, Day B. The role of *NDR1* in pathogen perception and plant defense signaling. Plant Signal Behav. 2011;6(8):1114–6.
41. Coppinger P, Repetti PP, Day B, Dahlbeck D, Mehlert A, Staskawicz BJ. Overexpression of the plasma membrane-localized NDR1 protein results in enhanced bacterial disease resistance in *Arabidopsis thaliana*. Plant J. 2004;40(2):225–37.
42. Éva C, Zelenyánszki H, Tömösközi-Farkas R, Tamás L. Transgenic barley expressing the *Arabidopsis AKR4C9* aldo-keto reductase enzyme exhibits enhanced freezing tolerance and regenerative capacity. S Afr J Bot. 2014;93:179–84.
43. Vemanna RS, Babitha KC, Solanki JK, Amarnatha Reddy V, Sarangi SK, Udayakumar M. Aldo-keto reductase-1 (*AKR1*) protect cellular enzymes from salt stress by detoxifying reactive cytotoxic compounds. Plant Physiol Bioch. 2017;113:177–86.
44. Guan X, Yu L, Wang A. Genome-wide identification and characterization of Aldo-Keto Reductase (*AKR*) gene family in response to abiotic stresses in *Solanum lycopersicum*. Int J Mol Sci 2023, 24(2).
45. Turóczy Z, Kis P, Török K, Cserháti M, Lendvai Á, Dudits D, Horváth GV. Overproduction of a rice aldo–keto reductase increases oxidative and heat stress tolerance by malondialdehyde and methylglyoxal detoxification. Plant Mol Biol. 2011;75(4):399–412.

46. Yue J, Liu J, Tang W, Wu YQ, Tang X, Li W, Yang Y, Wang L, Huang S, Fang C, Zhao K, Fei Z, Liu Y, Zheng Y. Kiwifruit Genome Database (KGD): a comprehensive resource for kiwifruit genomics. Hortic Res. 2020;7(1):117.
47. Tang W, Sun X, Yue J, Tang X, Jiao C, Yang Y, Niu X, Miao M, Zhang D, Huang S, Shi W, Li M, Fang C, Fei Z, Liu Y. GigaScience. Chromosome-scale genome assembly of kiwifruit *Actinidia eriantha* with single-molecule sequencing and chromatin interaction mapping. 2019, 8(4).
48. Letunic I, Bork P. 20 years of the SMART protein domain annotation resource. Nucleic Acids Res. 2018;46(D1):D493–6.
49. Tamura K, Stecher G, Kumar S. MEGA11: molecular evolutionary genetics analysis version 11. Mol Biol Evol. 2021;38(7):3022–7.
50. Chen C, Chen H, Zhang Y, Thomas HR, Frank MH, He Y, Xia R. TBtools: an integrative toolkit developed for interactive analyses of big biological data. Mol Plant. 2020;13(8):1194–202.
51. Bailey TL, Boden M, Buske FA, Frith M, Grant CE, Clementi L, Ren J, Li WW, Noble WS. MEME SUITE: tools for motif discovery and searching. Nucleic Acids Res. 2009;37:W202–208.
52. Magali L, Patrice D, Gert T, Kathleen M, Yves M, Yves VDP, Pierre R, Stephane R. PlantCARE, a database of plant cis-acting regulatory elements and a portal to tools for in silico analysis of promoter sequences. Nucleic Acids Res 2002(1):1.
53. Horsch RB, Fry JE, Hoffmann NL, Wallroth M, Eichholtz D, Rogers SG, Fraley RT. A simple and general method for transferring genes into plants. Science. 1985;227(4691):1229–31.
54. Wang T, Karunairetnam S, Wu R, Wang Y-Y, Gleave AP. High efficiency transformation platforms for kiwifruit (*Actinidia* spp.) functional genomics. Acta Hortic. 2012;929:143–8.
55. Sun LM, Fang JB, Zhang M, Qi XJ, Chen JY. Molecular cloning and functional analysis of the *NPR1* homolog in kiwifruit (*Actinidia Eriantha*). Front Plant Sci. 2020;11:551201.
56. Chen Q, Wei T. Membrane and nuclear yeast two-hybrid systems. In: Plant Virology: Methods and Protocols. 2022: 93–104.
57. Zhang H, Cheng G, Yang Z, Wang T, Xu J. Identification of sugarcane host factors interacting with the 6K2 protein of the sugarcane mosaic virus. Int J Mol Sci 2019, 20(16).

Publisher's note